is less satisfactory. No explanation for the latter discrepancy has been advanced.

The facts that the average kinetic energy release values indicate that there is little or no reverse activation barrier for dissociation of thiophene to $C_2H_2S^+$ and C_2H_2, and the loose thiovinyl ketene transition state as indicated by the RRKM calculations leads us to postulate linear structure III for the $C_2H_2S^+$ fragment. In order to investigate this further, we performed ab initio calculations by using a Gaussian 70 program with the extended splitvalence 4-31G basis set[44] on the linear and cyclic structures for $C_2H_2S^+$. By optimizing geometries for the two structures, we found total energy minima for both structures. These calculations indicate that the linear structure is indeed more stable than its cyclic counterpart by 1.1 eV. This is contrary to previously assumed cyclic structure (II) of $C_2H_2S^+$.[45]

The possibility that the thiophene parent ion isomerizes to a more stable linear structure was considered. Two points argue against such a structure. First, ab initio calculations on the thiophene and thiovinyl ketene structures indicate that the thiophene ion is far more stable than the thiovinyl ketene ion. Second, a lower parent ion energy would have the effect of raising the activation energy, thereby increasing the parent ion density of states (denominator in eq 1). In addition, the lower vibrational frequencies of a linear structure would further increase the density of states. The net result would be to lower the RRKM calculated rate by over 2 orders of magnitude, contrary to the experimental results.

(43) H. M. Rosenstock, R. Stockbauer, and A. C. Parr, *J. Chem. Phys.*, **71**, 3708 (1979).
(44) R. Ditchfield, W. J. Hehre, and J. A. Pople, *J. Chem. Phys.*, **54**, 724 (1971). QCPE program No. 234.
(45) H. Budzikiewicz, C. Djerassi, and D. H. Williams, "Mass Spectrometry of Organic Compounds", Holden-Day, San Francisco, 1967.

Conclusion

A thermochemical onset for the dissociation of $C_4H_4S^+$ to $C_2H_2S^+$ and C_2H_2 measured by the kinetic energy release as a function of excess $C_4H_4S^+$ internal energy has been used to establish a 298 K heat of formation of the $C_2H_2S^+$ ion of 253 ± 3 kcal/mol. Comparison of the experimentally determined decay rates as a function of $C_4H_4S^+$ internal energy with calculated rates based on the statistical RRKM theory indicates that the parent ion structure is that of thiophene while the transition state is a loose structure such as thiovinyl ketene. Under these assumptions, there is excellent agreement between experimentally measured and the RRKM-calculated decay rates. These rates are significantly lower than those measured by Andlauer and Ottinger. The average kinetic energy releases as a function of ion internal energy increase monotonically with energy as expected on the basis of the statistical theory. However, the magnitude is significantly greater than predicted.

Acknowledgment. This work received support from the National Science Foundation. We thank Dr. Ron Hass for providing us with the MIKES kinetic energy release data.

Thermochemistry and Dissociation Dynamics of State-Selected C_4H_4X Ions. 2. Furan and 3-Butyn-2-one

Gary D. Willett[1] and Tomas Baer*

Contribution from the Department of Chemistry, The University of North Carolina at Chapel Hill, Chapel Hill, North Carolina 27514. *Received January 31, 1980*

Abstract: The photoion-photoelectron coincidence technique has been used to investigate the unimolecular decomposition mechanism of metastable state-selected furan and 3-butyn-2-one ions. Threshold photoelectron spectra and photoionization efficiency curves for the various fragment ions as well as fragment ion time-of-flight distributions are presented. From a comparison of the measured and statistically calculated absolute unimolecular dissociation rates, together with evidence from an independent study on the kinetic energy releases of a variety of $C_4H_4O^+$ isomers, it is concluded that at low internal energies the furan ion dissociates to $C_3H_4^+$, $C_2H_2O^+$, and $C_3H_3^+$ directly or possibly via a rate-determining isomerization. It is further shown that 3-butyn-2-one(1+) dissociates directly without first isomerizing to the more stable furan(1+) ion. The first and major product is $CHCCO^+$ whose ΔH_{f298K} is calculated to be 232 kcal mol^{-1}. Gaussian 70 4-31G ab initio MO calculations have been used to calculate the relative stabilities of various $C_4H_4O^+$ and $C_2H_2O^+$ structures.

I. Introduction

In 1971, Derrick et al.[2] reported the charge-exchange mass spectra of furan for primary ions of several recombination energies. In that experiment, charge transfer between a simple ion and the furan molecule results in the production of energy-selected furan ions. That study established that in the energy range 11-12 eV furan dissociates via three paths which are

$$C_4H_4O^+ \rightarrow C_3H_4^+ + CO \quad (1)$$

$$C_4H_4O^+ \rightarrow C_2H_2O^+ + C_2H_2 \quad (2)$$

$$C_4H_4O^+ \rightarrow C_3H_3^+ + CHO \quad (3)$$

Other reaction products observed at higher energy were $C_4H_3O^+$ and HCO^+.

In the charge-transfer preparation, ions are formed in relatively narrow and well-determined internal energies. For this reason, the charge-transfer mass spectra as a function of the ionizing energy constitute a breakdown diagram, which gives directly the relative rates for dissociation to the various fragments as a function of the parent ion internal energy. Insight into the dissociation dynamics can often be obtained by comparing experimental breakdown diagrams to those predicted by a theory, particularly the statistical theory of unimolecular decay (RRKM[3a] or QET[3b]). The input required for such calculations are dissociation onsets and vibrational frequencies and moments of inertia of the mo-

(1) Commonwealth Scientific Industrial Research Organization Postdoctoral Research Fellow, 1978.
(2) P. J. Derrick, L. Åsbrink, O. Edquist, B.-Ö. Jonsson, and E. Lindholm, *Int. J. Mass Spectrom. Ion Phys.*, **6**, 161 (1971).
(3) (a) R. A. Marcus and O. K. Rice, *J. Phys. Colloid Chem.*, **55**, 894 (1951); (b) H. B. Rosenstock, M. B. Wallenstein, A. L. Wahrhaftig, and H. Eyring, *Proc. Natl. Acad. Sci. U.S.A.*, **38**, 667 (1952).

0002-7863/80/1502-6769$01.00/0

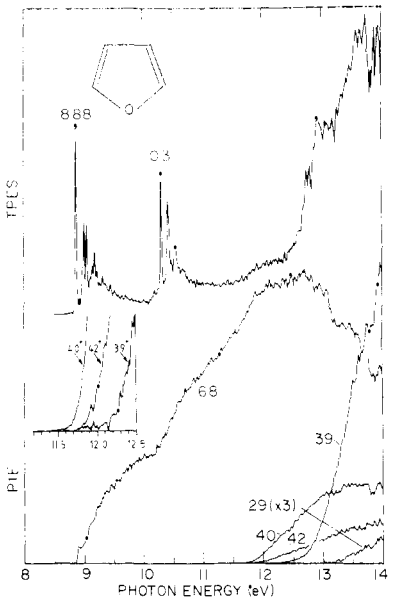

Figure 1. Threshold photoelectron spectrum (TPES) of furan and the photoionization efficiency (PIE) curves for the parent ion $C_4H_4O^+$ (m/e 68) and fragment ions $C_2H_2O^+$ (m/e 42), $C_3H_4^+$ (m/e 40), $C_3H_3^+$ (m/e 39), and HCO^+ (m/e 29).

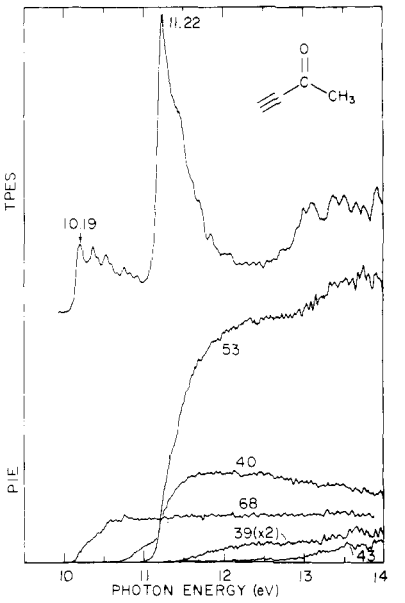

Figure 2. Threshold photoelectron spectrum (TPES) of 3-butyn-2-one, and the photoionization efficiency (PIE) curves for the parent ion $C_4H_4O^+$ (m/e 68) and fragmentations $CHCCO^+$ (m/e 53), CH_3CO^+ (m/e 43), $C_3H_4^+$ (m/e 40), $C_3H_3^+$ (m/e 39), and CHO^+ (m/e 29).

lecular ions and transition states for each dissociation channel. Although the charge-transfer experiments of Derrick et al.[1] produced ions in selected energies, only a limited number of primary ions, and therefore energies, were available. As a result, the dissociation onsets could not be determined with sufficient accuracy to carry out meaningful calculations with the statistical theory.

Recently Holmes and Terlouw[4] and Terlouw et al.[5] measured the kinetic energy released in the CO loss channel for a variety of metastable isomers of furan. They found that furan itself dissociates to $C_3H_4^+ + CO$ with a two component energy release. Of particular interest is that the various isomers investigated had different kinetic energy releases, suggesting that isomerization among the various isomers is hindered.

In addition to the kinetic energy release results, Holmes and Terlouw[4] also reported on the thermochemistry of the neutral and ionic isomers of furan. The vinyl ketene ion was found to be more stable than the furan ion.

We have investigated a number of isomeric systems by photoion–photoelectron coincidence (PIPECO), among which are $C_4H_6^+$,[6] $C_4H_8^+$,[7] $C_6H_6^+$,[8] and $C_8H_8^+$,[9] and have found that the isomerization reactions yielding parent ions in their lowest energy configuration are much faster than the dissociation steps. However on the basis of metastable ion studies in conventional mass spectrometers, other workers[10] have concluded that in some closed-shell ions such as $C_3H_7O^+$, $C_3H_9O^+$, $C_3H_8N^+$, and $C_4H_{10}N^+$, isomerization is the rate-limiting step, rather than dissociation.

The experimental procedure used in this work has been described in paper 1 of this series.[11] The C_4H_4O samples were purchased from Aldrich. The furan contained no detectable impurities as determined by photoionization mass spectrometry, while the 3-butyn-2-one contained a trace of 3-buten-2-one. However, it was used without further purification.

II. Results

(A) Threshold Photoelectron Spectra. (i) Furan. The furan threshold photoelectron spectrum (TPES) over the 8–14-eV ionization energy range is shown in Figure 1. Previous experimental and theoretical studies on the electronic structure of furan reveal that there are four electronic ion states, $1a_2$ (π, 8.9 eV), $2b_1$ (π, 10.3 eV), $6a_1$ (σ, 13.0 eV), and $5a_1$ (σ, 13.8 eV), that are accessible to 8–14-eV radiation.[12] A comparison between the present TPES and earlier He I spectra[12] shows the same overall spectral features and ionization energies. The only major difference between the two spectra is that there is electron signal in the Franck-Condon gaps of the first three bands of the TPES. Structure such as this has been previously reported for a variety of compounds and is associated with resonant autoionization which forms ions in highly excited vibrational and rotational states.[13,14]

The high-energy Rydberg transitions of furan have been discussed in detail by Derrick and co-workers.[2] They have assigned the broad bands at ~10.9 and ~14 eV in previously reported UV absorption spectra of Sallavanti and Fitts[15] and Watanabe and Nakayama[16] as arising from several Rydberg series which converge to the $2b_1$ and $6a_1/5a_1$ molecular ion states. The same Rydberg series are most likely responsible for the increased electron structure over the 11–13-eV ionization energy range in the TPES. Such Rydberg transitions are of benefit to the PIPECO experiment since they provide a pathway for the formation of ions of nearly every energy.

(ii) 3-Butyn-2-one. The TPES of 3-butyn-2-one is shown in Figure 2. The ionization energy of 10.19 ± 0.01 eV is lower than a recent[17] He I determination of 10.25 eV. Our value is calibrated against the wavelength of the Lyman-α peak in the dispersed photon source and is in no manner influenced by such factors as electrode contact potentials. The first two bands can be assigned fairly convincingly by analogy with acetone and acetylene. The

(4) J. L. Holmes and J. K. Terlouw, *J. Am. Chem. Soc.*, **101**, 4973 (1979).
(5) J. K. Terlouw, P. C. Burger, and J. L. Holmes, *J. Am. Chem. Soc.*, **101**, 225 (1979).
(6) A. S. Werner and T. Baer, *J. Chem. Phys.*, **62**, 2900 (1975).
(7) T. Baer, D. Smith, B. P. Tsai, and A. S. Werner, *Adv. Mass Spectrom.*, **7A**, 56 (1978).
(8) T. Baer, G. D. Willett, D. Smith, and J. S. Phillips, *J. Chem. Phys.*, **70**, 4076 (1979).
(9) D. Smith, T. Baer, G. D. Willett, and R. C. Ormerod, *Int. J. Mass Spectrom. Ion Phys.*, **30**, 155 (1979).
(10) (a) R. D. Bowen and D. H. Williams, *J. Am. Chem. Soc.*, **99**, 5481, 6822 (1977); **100**, 7454 (1978); (b) *J. Chem. Soc., Perkin Trans. 2*, 68 (1978).
(11) J. J. Butler and T. Baer, *J. Am. Chem. Soc.*, preceding paper in this issue.
(12) W. Von Niessen, W. P. Kraemer, and L. S. Cederbaum, *J. Electron Spectrosc. Relat. Phenom.*, **8**, 179 (1976), and references cited therein.
(13) P. T. Murray and T. Baer, *Int. J. Mass. Spectrom. Ion Phys.*, **30**, 165 (1979).
(14) T. Baer, P. M. Guyon, I. Nenner, A. Tabché-Fouhaillé, R. Botter, L. F. A. Ferreira, and T. Govers, *J. Chem. Phys.*, **70**, 1585 (1979).
(15) R. A. Sallavanti and D. D. Fitts, *Int. J. Quantum Chem.*, **3**, 33 (1969).
(16) K. Watanabe and T. Nakayama, *J. Chem. Phys.* **29**, 48 (1958).
(17) J. L. Holmes, J. K. Terlouw, P. C. Vijfhuizen, and C. A'Compo, *Org. Mass. Spectrom.*, **14**, 204 (1979).

Table I. Fragment Appearance Energies

fragments	exptl AE, eV	thermochemical[a] AE, eV
Furan (IE = 8.88 eV)		
$C_2H_2O^+ + C_2H_2$	11.80 ± 0.10	11.70
$C_3H_4^+ + CO$	11.60 ± 0.10	10.88 (allene)
		11.49 (propyne)
$C_3H_3^+ + CHO$	12.10 ± 0.10	11.85
$CHO^+ + C_3H_3$	13.2 ± 0.1	12.32
3-Butyne-2-one (IE = 10.19 eV)		
$C_3HO^+ + CH_3$	11.00 ± 0.10	*b*
$CH_3CO^+ + C_2H$	12.10 ± 0.10	10.97
$C_3H_4^+ + CO$	10.68 ± 0.05	10.61 (propyne)
$C_3H_3^+ + CHO$	11.55 ± 0.10	10.97

[a] The following $\Delta H_f^\circ_{300K}$ in kcal/mol were used: C_4H_4O [furan] (−8.3);[20] C_4H_4O [3-butyne-2-one] (12);[4] CH_2CO^+ (207.3);[20] C_2H_2 (54.2);[20] $C_3H_4^+$ [allene] (269);[20] $C_3H_4^+$ [propyne] (283);[20] CO (−26.4);[20] $C_3H_3^+$ (256);[8] CHO (9);[21] CHO^+ (195);[20] C_3H_3 (81);[20] CH_3 (34);[20] CH_3CO^+ (151);[20] C_2H (114).[20] [b] Derived ΔH_f° for $CHCCO^+$ is 232 kcal/mol.

oxygen one-pair electron in acetone is the highest lying orbital, and its removal gives acetone an ionization energy of 9.72 eV. This is close to the 10.19 eV for 3-butyn-2-one. In addition, the vibrational spacing of 1250 cm^{-1} is very close to a progression in acetone with a spacing of 1210 cm^{-1} assigned by Brundle et al.[18] to a methyl group symmetric deformation mode. We therefore assign the first band to the removal of an oxygen lone-pair electron.

The second band can be attributed to the removal of one of the acetylene π electrons. The first band of acetylene itself has an ionization energy of 11.41 eV and a vibrational progression of 1830 cm^{-1}.[19] These two values are very close to the ionization energy of 11.22 eV and a poorly resolved vibrational progression with a spacing of approximately 1800 cm^{-1}. Because the resolution of the spectrometer is on the order of 25 meV (200 cm^{-1}), it is evident that the excitation of other vibrations causes this second band, as well as the first, to be poorly resolved.

(B) Photoionization Efficiency Curves. (i) Furan. The photoionization efficiency (PIE) curves for furan over the 8–14-eV range are shown in Figure 1. Fragment ion appearance energies and thermochemical onsets for $C_2H_2O^+$, $C_3H_4^+$, $C_3H_3^+$, and HCO^+ are listed in Table I. It is of interest that the experimental onsets for masses 42, 40, and 39 occur in the Franck–Condon gap region of 11–12 eV and are considerably lower than the corresponding values reported in earlier charge-exchange measurements.[2]

Above the first fragmentation onset, the parent ion yield curve is expected to be flat if direct ionization dominates the ion formation process. However for furan in the region between 12 and 14 eV, the previously mentioned autoionization causes the parent ion curve to have a peak. This peak is just at the maximum in the autoionization band in the TPES.

Examination of the experimental and thermochemical fragmentation onsets listed in Table I reveals that the experimental onset for $C_3H_4^+$ (allene) is 0.70 eV above its thermochemical dissociation limit. That the $C_3H_4^+$ ion structure from furan is propyne, whose onset nearly coincides with the one experimentally observed, was considered. There is no simple mechanism for the production of either allene or propyne from furan. In addition, the reaction rate is slow (see following section). Under these conditions, it is most reasonable that the lowest energy $C_3H_4^+$ structure is in fact produced. However, the 2- (or more) component kinetic energy release[4,5] may indicate that the dissociation proceeds via 2 or more paths.

Scheme I

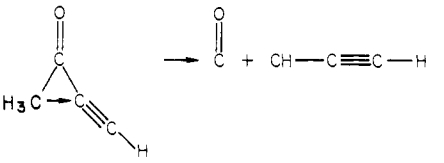

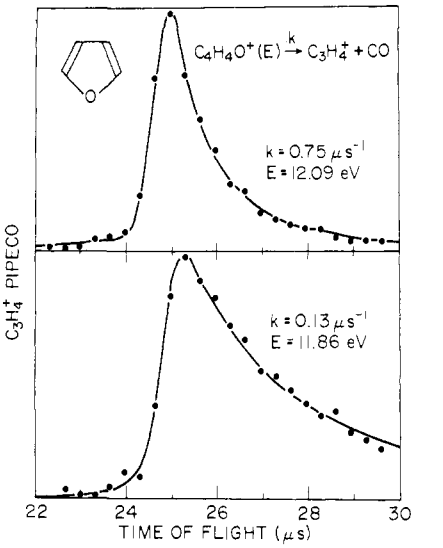

Figure 3. Representative coincidence time-of-flight distributions for the $C_3H_4^+$ fragment produced from state selected $C_4H_4O^+$ at the two indicated photon energies. The solid lines represent the calculated time-of-flight distributions determined by using the indicated fragmentation rates, *k*.

A striking feature of the ion yield curves is the almost continuously increasing intensity of the $C_3H_3^+$ fragment. By 14 eV, this ion is the most abundant fragment and has an intensity equal to that of the parent.

(ii) 3-Butyn-2-one. The PIE curves for 3-butyn-2-one are shown in Figure 2, and the derived onsets for the fragments $C_3H_4^+$, C_3HO^+, $C_2H_3O^+$, and $C_3H_3^+$ are listed in Table I. The fragments observed for this ion are very different from those of furan. In 3-butyn-2-one, mass 42 is absent while mass 53 (not observed in furan) is the most abundant fragment between 11 and 14 eV. The heat of formation of neutral 3-butyn-2-one is estimated from group additivity relations to be 12 kcal/mol.[4] With use of this value, thermochemical onsets for the various fragments can be calculated. The onset for mass 40 ($C_3H_4^+ + CO$) at 10.68 eV is consistent with the formation of the methylacetylene ion (10.61 eV). The methylacetylene structure can be easily formed by the displacement of the CO molecule by the CH_3 group as shown in Scheme I. However, we cannot rule out the production of allene(1+).

It can be expected that the simple bond rupture to yield $HC{\equiv}C{-}CO^+ + CH_3$ has an onset at its thermochemical dissociation limit because such dissociations usually do not involve significant reverse activation barriers. Using a ΔH_f° (CH_3) of 34 kcal/mol, we calculate a ΔH_f° ($HC{\equiv}C{-}CO^+$) of 232 kcal/mol.

(C) Unimolecular Dissociation Rates. Only the furan ion was found to be metastable. Figure 3 illustrates two representative coincidence TOF distributions for the $C_3H_4^+$ fragment at two different photon energies. Only two spectra are shown here since the other TOF distributions are similar to these. Asymmetric TOF distributions were also recorded for $C_2H_2O^+$ and for the same reason these spectra are not reproduced here.

The solid lines shown in Figure 3 represent calculated TOF distributions determined by using the indicated fragmentation rates. These calculated TOF distributions are fitted to the experimental data by using ion acceleration and drift distances, the acceleration field, and the fragment and parent masses. The one adjustable parameter is the mean ion lifetime. Kinetic energy release and other TOF-broadening sources (e.g., the quadrupole

(18) C. R. Brundle, M. B. Robin, N. A. Kuebler, and H. Basch, *J. Am. Chem. Soc.*, 94, 1451 (1972).
(19) D. W. Turner, C. Baker, A. D. Baker, and C. R. Brundle, "Molecular Photoelectron Spectroscopy", Wiley-Interscience, London, 1970.
(20) H. M. Rosenstock, K. Draxl, B. W. Steiner, and J. T. Herron, *J. Phys. Chem. Ref. Data*, 6 (1) (1977).
(21) S. W. Benson in "Thermochemical Kinetics", Wiley-Interscience, New York 1976.

Table II. PIPECO Branching Ratios and Experimental Total Fragmentation Rates for Furan(1+)

total energy,[a] eV	total decay rate, μs^{-1}	branching ratios		
		$C_3H_3^+$	$C_3H_4^+$	$C_2H_2O^+$
11.27	0.03		1	
11.40	0.07		1	
11.50	0.13		1	0.01
11.62	0.32		1	0.17
11.73	0.75	0.01	1	0.26
11.98	5.1[b]	0.02	1	0.32

[a] Total energy = photon energy + ΔH_f°(furan). [b] This decay rate was determined by a straight line extrapolation of the lower energy decay rates, but the branching ratios are direct measurements.

mass filter) are accounted for by convoluting the calculated TOF distribution by a broadening function. This approach is considerably faster but indistinguishable from the more exact method of summing over a distribution of kinetic energy releases and ion lifetimes, especially in the case of a small kinetic energy release such as that in the furan(1+) dissociation.

A small correction is needed to account for the contamination of the ion energy selection by hot electrons which pass through the collimated hole structure. Such corrections reduce the measured lifetimes by <30%.

For all photon energies investigated, the measured rates for the production of $C_3H_4^+$ and $C_2H_2O^+$ were identical. This result indicates that reactions 1 and 2 are in competition over the metastable energy range of 11.5–13 eV. Because of the higher appearance energy and lower signal intensity for the $C_3H_3^+$ ion, it was not possible to confirm experimentally that this reaction channel was also in competition with channels 1 and 2.

If we do assume that reaction channels 1–3 are in competition over the metastable energy range, then the PIPECO branching ratios together with the measured total decay rates listed in Table II can be used to determine the absolute reaction rates for each of these channels in the following fashion. In the PIPECO experiment, we measure k_T, the total rate of disappearance of $C_4H_4O^+$, via reactions 1–3. For the pressures used in the experiment, we can neglect the contributions of collisional stabilization and bimolecular reactions of $C_4H_4O^+$ as sources of its depletion. We also assume that there is no fluorescence stabilization of the parent ions. The rate of $C_4H_4O^+$ depletion then is represented by

$$\frac{d[C_4H_4O^+]^*}{dt} = -k_T[C_4H_4O^+]^* \quad (4)$$

and if reaction channels 1–3 are in competition

$$k_T = k_{39} + k_{40} + k_{42} \quad (5)$$

where k_{40}, k_{42}, and k_{39} represent the respective unimolecular rate constants for reactions 1–3.

If eq 5 is then combined with the ratios R_1 and R_2, where I_{39},

$$R_1 = I_{42}/I_{40} = k_{42}/k_{40}$$

$$R_2 = I_{39}/I_{40} = k_{39}/k_{40} \quad (6)$$

I_{40}, and I_{42} are the intensities for $C_3H_3^+$, $C_3H_4^+$, and $C_2H_2O^+$ listed in Table II, the absolute rates k_{39}, k_{40}, and k_{42} can be evaluated. The experimental rates determined in this fashion are plotted as a function of $C_4H_4O^+$ internal energy in Figure 4.

III. Discussion

(A) Comparison of Furan and 3-Butyn-2-one Dissociations. All previous isomeric systems studied by us,[6-9] as well as four isomers of pyrrole,[22] isomerize more rapidly than they dissociate. That this is not the case with furan and 3-butyn-2-one is evident from the PIE curves as well as the lack of metastable 3-butyn-2-one

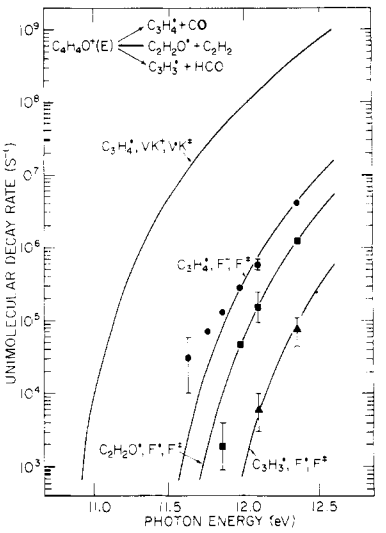

Figure 4. Experimental and RRKM calculated unimolecular fragmentation rates for furan versus photon energy. The points (■) $C_3H_4^+$, (●) $C_2H_2O^+$, and (▲) $C_3H_3^+$ represent the experimental rates determined from the total dissociation rates and PIPECO branching ratios listed in Table II. Competition between the $C_3H_4^+$, $C_2H_2O^+$, and $C_3H_3^+$ channels is assumed. The solid and dashed lines represent RRKM-calculated rates for the various product channels where the identifying letters indicate the assumed structures of the molecular ion (+) and transition state (‡) and F = furan and VK = vinyl ketene.

ions. The direct fragmentation path of 3-butyn-2-one to give CH_3 and HC≡C—C$^+$=O is absent in furan even at the highest energy investigated. This indicates that the dissociation paths of these two ions do not pass through a common part of their phase space. On the other hand, the collisional activation spectra[4] of furan and vinyl ketene are somewhat similar especially in their conspicuous absence of mass 53 (HC≡C—C$^+$=O). These data are consistent with a mechanism in which furan ions isomerize to a structure such as vinyl ketene prior to dissociation. However in view of the kinetic energy release and our lifetime measurements, other mechanisms may also be possible.

(B) Kinetic Energy Release. An RRKM calculation shows that the 0.70-eV difference between the experimental and thermodynamic dissociation onsets for CO loss cannot be due entirely to kinetic shift (the shift of the onset to an energy sufficiently high so that the rate of dissociation is greater than about 10^{+5} s^{-1}). Therefore if the product ion has the allene structure, a considerable portion of this 0.70 eV must be a result of a reverse activation barrier. Holmes and Terlouw[4] have measured the kinetic energy release distribution in furan. Their results indicate that somewhat less than half of the dissociations are accompanied by a release energy of about 25 meV. The rest is associated with a broad distribution of release energies extending to 0.3 eV. By contrast, the more stable isomer vinyl ketene(1+) dissociates with a Gaussian distribution whose average kinetic energy is 60 meV. On the basis of these results, it is not possible to generate a unique mechanism for the dissociation of furan ions. There may be two or more dissociation paths, one of which produces methylacetylene(1+) with little release energy, while another produces allene(1+) via some $C_4H_4O^+$ isomer.

(C) Comparison of the Decay Rates with the Statistical Theory. Using the thermochemical results summarized in Table I, it is possible to compare our measured decay rates with those predicted by the statistical theory (Bunker–Hase RRKM program).[23]

In carrying out the calculation, we must decide whether the rate-determining step is the isomerization or direct dissociation from furan or the dissociation of an isomerized species such as vinyl ketene to $C_3H_4^+$ + CO. The major difference is in the activation energy. In the former case, it is the appearance energy − ionization energy − kinetic shift = 2.72 eV − kinetic shift, and

(22) G. D. Willett and T. Baer, *J. Am. Chem. Soc.*, following paper in this issue.

(23) Available as program 234 through the Quantum Chemistry Program Exchange, Indiana University.

Table III. Vinyl Ketene Molecular Ion Fundamental Vibrational Frequencies Used in the RRKM Calculations (in cm^{-1})[a]

C–H stretch	3118, 3102, 3028, 3000
C–C stretch and torsion	1158, 157
C=C, C=O stretch	1388, 1625,[b] 2151
CH_2 scissors, rock, wag, and twist	1420, 912, 959, 593
CH bends	1275, 1275, 993, 993
CCC, CCO, and CCCCO bend, torsion, and deformation	528, 438, 327, 100

[a] Normal-mode frequencies are estimated from those of the related molecules propenal and ketene given in ref 25 and 24, respectively. [b] Assumed reaction coordinate.

in the latter, it is 2.11 eV. The available energy ($h\nu$ – ionization energy) is approximately the same because the heats of formation of furan(1+) and vinyl ketene(1+) ions are very similar. We performed both calculations. For the case in which the rate-determining step is the dissociation of vinyl ketene(1+), we used an activation energy of 2.11 eV and the vibrational frequencies of vinyl ketene for both the molecular ion and the transition state in the RRKM calculation. The vibrational frequencies of vinyl ketene(1+) are unknown and were therefore estimated from the related molecules ketene[24] and propenal.[25] These are listed in Table III. This calculation results in rates given in Figure 4 as $C_3H_4^+$, VK^+, $VK^‡$. Clearly these rates are far too high.

We therefore conclude that the rate-determining step for $C_3H_4^+$ formation is not the dissociation form vinyl ketene(1+). For the contrary assumption, that furan dissociates directly or undergoes a rate-determining isomerization, we used an activation energy of 2.64 eV. This value has adjusted somewhat to take into account the kinetic shift which we determine to be 0.1 eV. The vibrational frequencies used are those of the furan molecule.[25] In large molecules such as furan, the vibrational frequencies of the ion are expected to be similar to those of the molecule so that the molecular ion density-of-states can be calculated with reasonable accuracy by assuming the molecular frequencies for the precursor ion.

The choice of frequencies for the transition state is more complicated since neither the structure nor the frequencies are amenable to experimental investigation. For dissociation reactions with little or no reverse activation energy, it is reasonable to propose a structure for the transition state which is similar to the final dissociated products.[26] On the other hand for dissociation reactions involving a large reverse activation barrier, it is expected that the transition state would involve a tight complex, and so for the present case, a furan transition state with the 603-cm^{-1} ring vibration chosen as a reaction coordinate was used.

The reaction to $C_3H_3^+$ and $C_2H_2O^+$ was assumed to proceed directly from the furan ion to the transition state and then to products. The contrary assumption, that all fragments are formed from an isomerized structure such as vinyl ketene, leads to a branching ratio between $C_3H_4^+$ and $C_3H_3^+$ or $C_2H_2O^+$ which is too high by nearly 3 orders of magnitude. For lack of additional information, we used furan vibrational frequencies for the molecular ion and transition states for $C_3H_3^+$ and $C_2H_2O^+$ formations as well.

A comparison of the RRKM calculated rates, assuming activation of 2.64, 2.76, and 2.98 eV for $C_3H_4^+$, $C_2H_2O^+$, and $C_3H_3^+$, respectively, with the experimental rates is presented in Figure 4. There is close agreement between the calculated (solid lines) and experimental (points) rates for reactions 1–3 when a furan molecular ion and a furan transition state were used.

A comparison of the calculated and measured rates for the HCO loss channel with the corresponding values for reaction 1 and 2 reveals that there is not a simple explanation for the steadily increasing $C_3H_3^+$ ion yield. Above ~13 eV, dissociation to produce $H_2C{-}C{\equiv}CH^+$ (thermochemical AE = 12.98 eV) could provide an increased $C_3H_3^+$ yield; however, between ~12.4 and ~13 eV, there must be a different mechanism to the one described for the metastable energy range.

(D) Structures of $C_4H_4O^+$ and $C_2H_2O^+$. In order to test the conclusion of Holmes and Terlouw[4] concerning the stability of vinyl ketene, we carried out some ab initio SCF Gaussian 70 4-31G calculations[27] on this as well as on the furan ion. All bond lengths and many angles were varied to obtain an optimized structure for vinyl ketene. Yet, the energy of the furan was found to be lower by about 9 kcal/mol (0.4 eV). However such calculations are probably not accurate to more than about 10 kcal/mol. Therefore, they are not inconsistent with the experimental results which are that vinyl ketene(1+) is 3 kcal/mol more stable than furan(1+).

A similar investigation concerning the ketene and cyclic structures of $C_2H_2O^+$ indicated that the ketene ion is more stable than its cyclic counterpart by over 2 eV. In addition, there is no experimental evidence that an ionic structure more stable than ketene exists.

IV. Conclusion

By considering the kinetic energy release measurements of Holmes and Terlouw and our absolute rate measurements at selected furan ion internal energies, we conclude that the furan ion dissociation is a complex one, possibly proceeding via parallel paths. However, the rate-determining step in the dissociation is the first one which takes the $C_4H_4O^+$ from the furan structure either to products directly or via some other isomeric structures. It is on account of the high barrier for isomerization that the other fragment ions $C_3H_3^+$ and $C_2H_2O^+$ are competitive with allene formation.

The furan ion dissociation is the first case which we have encountered in which isomerization is slower than the subsequent dissociation. In addition, 3-butyn-2-one, an isomer of furan, dissociates directly without isomerizing even at low energies. This state of affairs is not something which can be attributed simply to the rigid nature of the furan and 3-butyn-2-one ions. Other rigid ions such as cyclobutene, 2,4-hexadiyne, and cyclooctatetraene are known to isomerize with rates greater than those for dissociation.

Acknowledgment. We are most grateful to Professor John Holmes for providing us with a preprint of his study on the structures and heats of formation of the $C_4H_4O^+$ ions prior to publication and for our illuminating discussions with him concerning the furan ion dissociation mechanism. We also thank Professor Lee Pedersen for help in carrying out the Gaussion 70 molecular orbital calculations. This work was supported by the National Science Foundation.

(24) A. P. Cox and A. S. Esbitt, *J. Chem. Phys.*, **38**, 1636 (1963).
(25) T. Shimanouchi, *Natl. Stand. Ref. Data Ser. (U.S. Natl. Bur. Stand.)*, 39 (1972).
(26) G. S. Hammond, *J. Am. Chem. Soc.* 77, 334 (1955).
(27) R. Ditchfield, W. J. Hehre, and J. A. Pople, *J. Chem. Phys.*, **54**, 724 (1971).